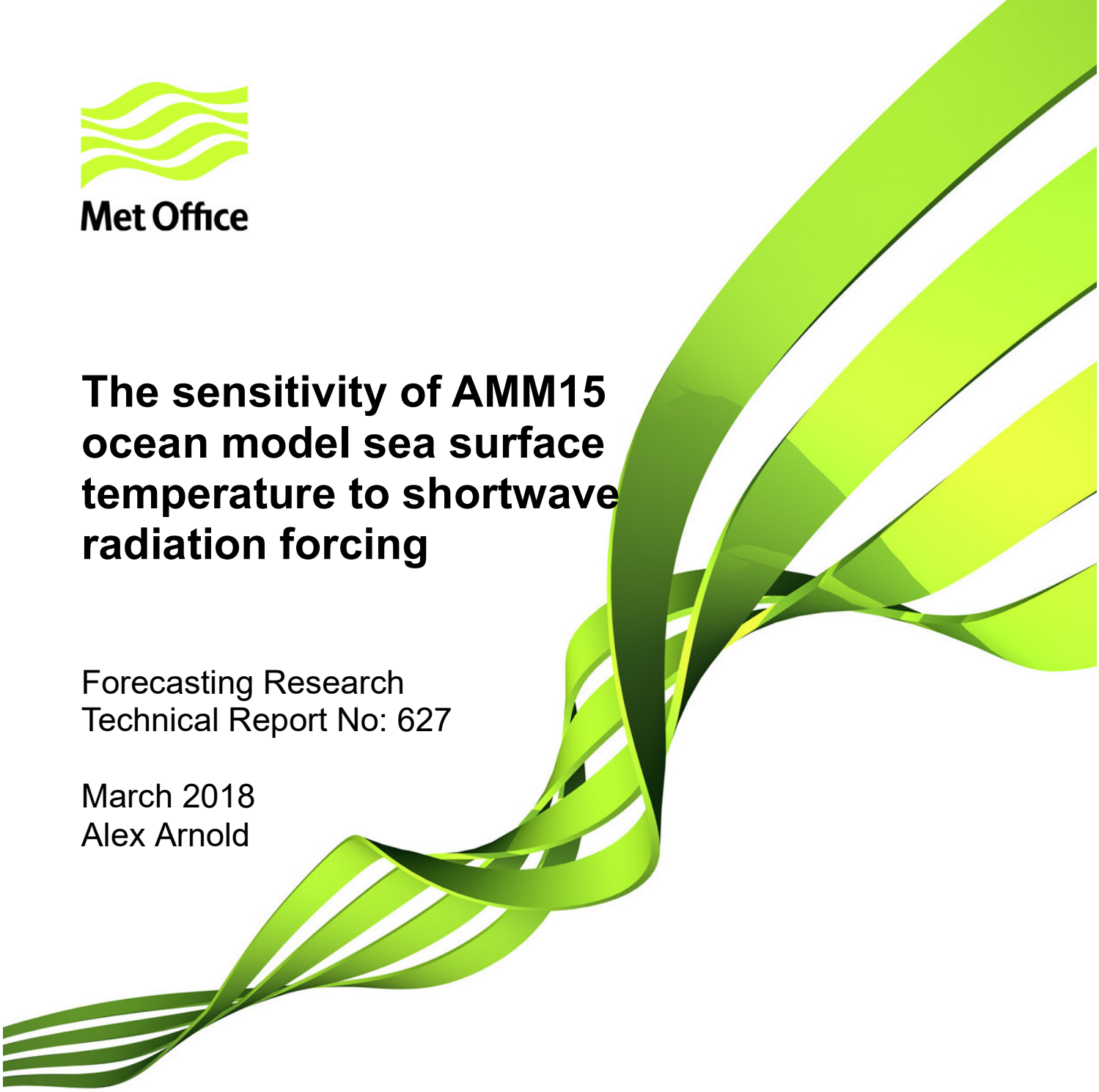

The sensitivity of AMM15 ocean model sea surface temperature to shortwave radiation forcing

Forecasting Research
Technical Report No: 627

March 2018

Alex Arnold

Contents

Summary

In this report, we investigate how different choices in specification of surface boundary conditions and the ratio of penetrating to non-penetrating shortwave solar radiation affect the AMM15 NEMO ocean model configuration sea surface temperature (SST). In shallow well mixed areas and close to the UK coast, overall the effect of changing this ratio is not very strong. However, further away from land, if the ratio specifies less penetrating radiation (larger 'R-value') warmer SSTs are produced in summer, with a corresponding cooling deeper in the water column. Winter SST results are shown to be insensitive to the choice of penetrating ratio. In general, the AMM15 SST is shown to have a slight cold bias relative to OSTIA and in-situ observations when it is forced using NWP fluxes specified with bulk CORE forcing. However, when it is forced using direct NWP fluxes, the AMM15 produces a warm SST bias in the tests conducted.

1. Introduction

The Atlantic Margin Model (AMM15) NEMO configuration has a horizontal resolution of 1.5 km and covers an area surrounding the UK and north-west Europe. This region includes the deep Atlantic waters to the west and shallow North West shelf seas in the east – in particular the North Sea, recognised as an area with turbid waters. This makes it difficult to choose a light scheme that accurately represents the attenuation of incident solar radiation across this domain. In this report, we investigate how best to treat the incident short wave radiation within the NEMO ocean model for AMM15, to give the most accurate Sea Surface Temperature (SST).

Solar radiation with wavelengths longer than 0.7 μm is absorbed in the top 50 cm of the ocean. More of the solar energy penetrates the ocean at wavelengths shorter than 0.7 μm. The treatment of this component of the incoming radiation in the NEMO ocean model is dependent on the light attenuation scheme chosen (Madec, 2008). Most models have a common first term to their formulations that describes the treatment of the non-penetrating light. How the penetrating part of the spectrum is treated is what differs.

Paulson and Simpson (1977) suggested a simple 2 band formulation where the first term deals with the non-penetrating fraction of light, and the second term describes the absorption over depth, of the penetrating light.

$$I(z) = Q_{SR}\left(Re^{-z/\xi_0} + \left((1-R)e^{-z/\xi_1}\right)\right) \quad (1)$$

Where *I(z)* is the downward irradiance of solar radiation, *z* is depth, Q_{SR} is the shortwave radiation, *R* is a constant specifying the fraction of non-penetrating light, ξ_0 specifies the very near surface depth of extinction and ξ_1 the depth of extinction for shorter wavelengths. Both ξ and R values are specific to water type (explained in Section 2.2).

Morel (1988) found this to be too simplistic a formulation, so developed a 61 waveband model dependent on the wavelengths of light, to more accurately represent the light absorption. Lengaigne et al. (2007) developed the “RGB scheme” (Equation 2) which is a simplification of the slightly modified 61 waveband model of Morel and Maritorena (2001), which was too computationally expensive. The RGB scheme splits the incoming visible light in to 3 bands representing blue (400-500nm), green (500-600nm) and red

(600-700nm) light, which is used in NEMO to describe the attenuation of incoming solar radiation.

$$I(z) = Q_{SR}\left(Re^{-z/\xi_0} + \left(\binom{(1-R)}{3}\left(e^{-z/rr} + e^{-z/gg} + e^{-z/bb}\right)\right)\right) \quad (2)$$

The coefficients *rr*, *gg* and *bb* are specific to each respective waveband and have the option of being chlorophyll dependent**,** which could help improve the accuracy of modelling the attenuation of incident radiation. For the global ocean, this was investigated by Ford and Barciela (2015). Currently in our tests, the chlorophyll is set to 0.05 mg/m^3 everywhere and so does not affect the coefficients by varying in time or space. At this chlorophyll concentration, coefficients rr, gg, bb are set to: 0.38189, 0.07866 and 0.02501 respectively here.

2. Method

The AMM15 configuration using NEMO version 3.6_stable (revision 6232) was run for two month-long simulations: December 2014 and June 2015. The model was forced using 1/12° NATL12 (Storkey et al. 2010) output for lateral boundaries and the surface meteorology forcing conditions were provided by the operational 17km horizontal resolution global Unified Model (Walters et al. 2014), referred to as NWP768. For more details on model set up, see Graham et al. (2018).

2.1 R-values

Paulson and Simpson (1977) derived a list of coefficients ("R-values") to specify the fraction of solar radiation that is absorbed at the surface and the fraction which penetrates. These were based on fitting the sum of the two exponentials in Equation 1 to observations of downward irradiance values of different Jerlov (1951) optical water types (explained in Section 2.2). These values however, are only valid over a specific set of wavelengths (0.4 – 1 μm).

In the UK Environmental Prediction regional coupled model configurations (Lewis et al. 2018), NEMO AMM15 is being run using the shortwave radiation provided by the NWP768 model. The shortwave radiation outputted by the NWP768 model is provided as either 0.2-1 μm, referred to as Band 1 (where light with wavelengths longer than 1 μm are added to the longwave radiation), and 0.2-10 μm, referred to as QTot. Therefore the R-values specified by Paulson and Simpson (1977) for the different water types are not directly applicable for use with the wavebands available to us from the Met Office Unified Model and equivalent R-values need to be calculated.

Previous analysis (John Edwards, pers. comm.) produced a breakdown of the percentages of incident solar radiation at different wavelengths in bands, shown in Table 1. Details are provided in Appendix 3.

Wavelength band (μm)	Percentage of light (TOA)
0.200 – 0.4	7.6%
0.400 – 0.689	37.6%
0.689 – 1	24%
1.000 – 10	30.6%

Table 1: Distribution of incoming (Top Of Atmosphere) solar radiation for different wavebands.

Using this information and the assumption that light with wavelengths longer than 0.7μm are non-penetrating, we can calculate the equivalent R-values for different water types. See Appendix 1 for an explanation of how this is calculated. Note that there is no account made in this analysis for the scattering or absorption of the incident radiation through the atmosphere.

2.2 Water Types

Jerlov (1951) classified water in to different 'Types' based on the vertical attenuation of spectral irradiance depending on water clarity. In older versions of the Forecasting Ocean Assimilation Model (FOAM, Bell et al. 2000), the Paulson and Simpson 2 band scheme (Equation 1) was used, with Jerlov Water Type IB (see Dave Storkey note from References). The R-value for this Water Type is 0.67, meaning that about 33% of the light penetrates (some of the 'non-penetrating' light does also penetrate slightly due to first term in Equation 2).

In NEMO, Water Type I is used, which has an assumed R-value of 0.58. In the Met Office, the global FOAM-NEMO models are using this Water Type, however as the AMM15 domain covers both deep ocean and shelf seas, this may not be the most suitable Water Type for this model. Due to the main area of interest being on the shelf and close to the coast, a Water Type which describes well mixed and turbid coastal waters and the North Sea (Jerlov Water Type III, Stip 2010) was one of the options tested. Table 2 summarises the Jerlov water types, R-values and equivalent R-values (due to how the shortwave radiation is provided by the NWP768 model) used in these tests. ξ_0 values specify the very near surface depth of extinction and are specific to water type.

	Paulson & Simpson values:		Equivalent R-values:	
Water type	ξ_0	R	R (Band 1)	R (QTot)
I	0.35	0.58	0.26	0.66
IB	1.0	0.67	0.38	0.72
III	1.4	0.78	0.53	0.79

Table 2: Summary of Paulson and Simpson R values for different water types and equivalent R values for use with NWP fluxes.

The sensitivity of ocean model results to using different R-values is expected to be more apparent in summer, when the daylight hours are longer and there is less reflection at the sea surface compared to in the winter when the sun is at a shallower angle. However to check this, the effect of different R-values on the model SST has been tested both in June 2015 and December 2014. R-values for Water Types I,IB and III were used. In addition to this, the difference between using QTot or the already partitioned Band 1 was investigated.

2.3 Forcing type

We also looked at the difference in schemes used to force the AMM15 at the surface. The two types tested were:

i) using directly prescribed fluxes from the Met Office Unified Model (MetUM) global NWP model (the method currently being used in the operational AMM7 model (O'Dea et al. 2012)),

ii) using the Common Ocean-ice Reference Experiment (CORE) bulk formulae (Large and Yeager 2009) to calculate sensible heat, momentum and evaporation from 'bulk' NWP quantities (temperature, wind, etc).

These tests were run for December 2014, in order to be able to compare results to a further simulation run by Jenny Graham (mi-am252_rnf), which used CORE bulk forcing but with ERA-Interim (Dee et al. 2011) fluxes rather than MetUM global NWP fluxes.

As the SSTs are different between an NWP model providing forcing and the ocean model, a correction term as suggested by Haney (1971) can applied, to relax the ocean model back towards a reference SST, provided by The Operational Sea Surface

Temperature and Sea Ice Analysis (OSTIA; Donolon et al. 2012). The effect of applying this correction is demonstrated in this study.

Table 3 contains a summary of the different tests carried out and for which months the tests were run.

Experiment	Model Description	Date
Forcing	ERA-Interim bulk	December 2014
	NWP bulk	December 2014, June 2015
	NWP direct; QTot	December 2014, June 2015
R value	NWP bulk; R=0.66	December 2014, June 2015
	NWP bulk; R=0.72	June 2015
	NWP bulk; R=0.79	December 2014, June 2015
	NWP direct; QTot; R=0.66	December 2014, June 2015
	NWP direct; QTot; R=0.72	December 2014, June 2015
	NWP direct; QTot; R=0.79	December 2014, June 2015
	NWP direct; QTot + Haney	December 2014, June 2015
SW partitioning	NWP direct; QTot; R=0.66	June 2015
	NWP direct; QTot; R=0.72	June 2015
	NWP direct; Band 1; R=0.26	June 2015
	NWP direct; Band 1; R=0.38	June 2015

Table 3: Summary of sensitivity tests carried out.

3. Results

The results from the tests conducted are presented in this Section. It should be noted that only the effect of changing these inputs on model SST is considered in detail in this Report, with no discussion of the accuracy of the model to simulate temperature at depth or other model diagnostics.

3.1 Forcing type

To investigate the effect of surface boundary condition forcing type used (bulk or direct), the AMM15 was run over the month of December 2014 using bulk forcing with ERA-Interim fluxes, bulk forcing with Met UM NWP fluxes and Direct QTot + Haney correction using NWP fluxes. All the model runs used equivalent R values (ERA-Interim forced model R=0.58, NWP forced models R=0.66).

Figure 1 shows a map of 'best suite' indicating which of the different forcing methods used in this study has the smallest RMSE at that site. It shows that using bulk forcing and NWP fluxes produces the more accurate SSTs relative to in-situ buoys compared to the other types of forcing tested at the majority of sites.

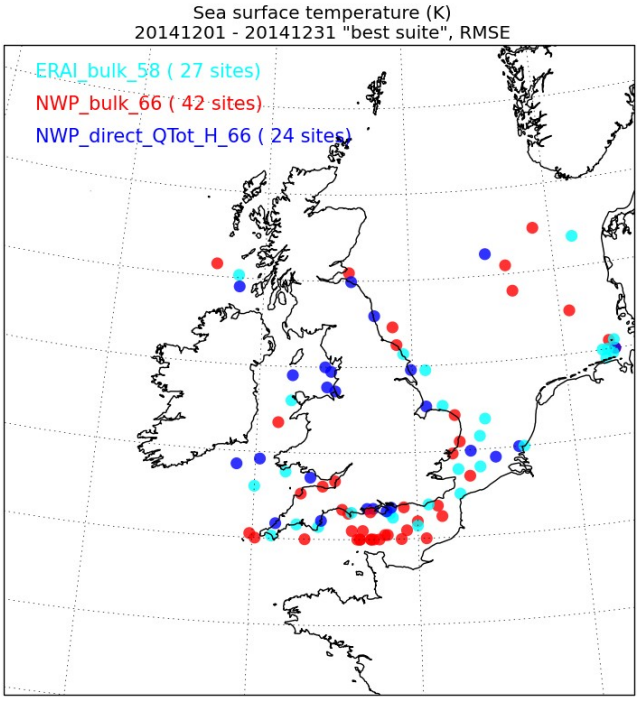

Figure 1. December 2014. Map of 'best suite' showing suite with smallest RMSE at each observation site. Cyan = ERAI bulk forcing, Red = NWP bulk forcing, Blue = NWP direct forcing with Haney.

Figure 2 shows an example time series at the EAOW observation site, located in the southern North Sea in a shallow well mixed area which does not stratify in summer. This demonstrates results found for a large proportion of the observation sites. Using ERA-Interim bulk forcing produces slightly too warm SSTs, as does the direct NWP forced model, whereas the bulk NWP forced model is slightly too cold relative to observations.

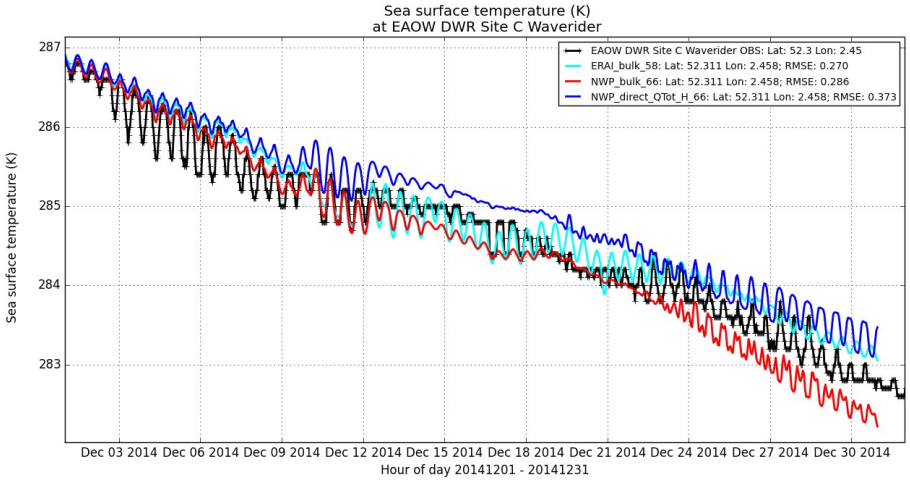

Figure 2. December 2014. Time series of SST at EAOW (Black). EAOW in Southern North Sea. Cyan = ERAI forced, Red = NWP bulk forced, Blue = NWP Direct QTot + Haney forced.

The differences in forcing types in comparison to OSTIA for the whole domain are shown in Figure 3. When considering the two CORE bulk forced setups (Figure 3a and Figure 3b), the SST difference compared to OSTIA is between $\pm$ 0.5K, however the ERA-Interim forced model (Figure 3a) has more of a warm bias than the NWP bulk forced model overall (Figure 3b). The direct forced NWP model also produces SSTs that are too warm (Figure 3c), especially on the shelf, and more so than with ERA-Interim.

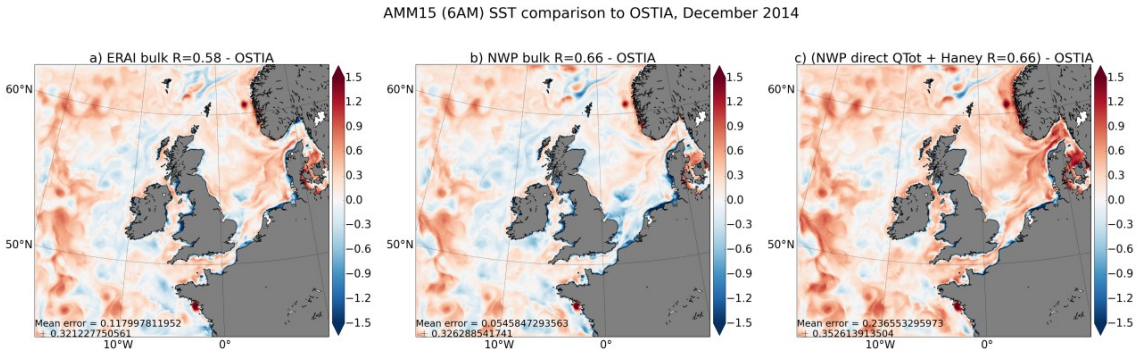

Figure 3. December 2014. Comparison to OSTIA. a) ERAI - OSTIA, b) NWP bulk - OSTIA, c) (NWP direct QTot+Haney) - OSTIA

Comparing the ERA-Interim to both NWP forced models (Figure 4), demonstrates how different surface forcing methods affect model SST, even when the fluxes originate from the same atmospheric model (Figure 4c). As shown in Figure 4a and Figure 4c, the AMM15 exhibits the overall pattern seen in previous plots, where the NWP bulk forced model is cooler than both the ERA-Interim and NWP direct forced models. When NWP direct forcing is used, the SST is warmer than OSTIA (as seen above in Figure 3) and warmer again than when forcing with ERA-Interim, as seen in Figure 4b. Using CORE bulk forcing results in cooler SSTs than when direct fluxes are applied as surface boundary conditions, especially on the shelf. The difference is shown in Figure 4c, where both NWP forced models, using R=0.66, are compared to each other.

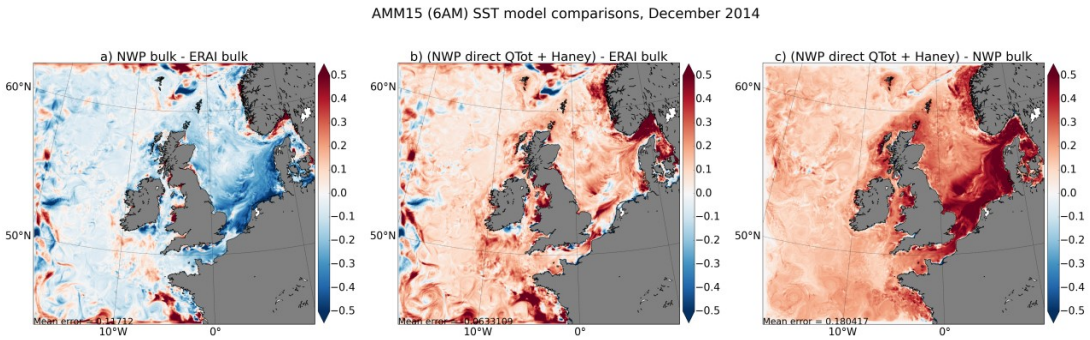

Figure 4. December 2014. a) NWP bulk - ERAI bulk, b) NWP direct - ERAI bulk, c) NWP direct - NWP bulk.

In the remainder of this Report, the fields used to force AMM15 are provided by the NWP768 global atmospheric MetUM model only. The following tests also focus on simulations for June 2015.

3.1.1 Haney correction

Figure 5 shows a time series plot at the Blackstones observation site in west Scotland, located in an area that is not excessively sheltered and is seasonally stratified. The difference between using bulk, direct QTot and direct QTot + Haney correction applied in June 2015 is demonstrated. The SST from using bulk forcing is closer to the observations (cyan line), although results from all observation sites suggest generally similar results achieved using the Direct QTot + Haney forcing. The configuration using direct forcing is much improved by adding Haney correction, given that it nudges the model SST towards an observed value. Overall, using direct forcing and applying Haney correction produces SSTs with lower RMSEs for June 2015 than when using bulk

forcing, due to it having a cold bias. The bulk forced run is relatively stable, but in summer it has a tendency to be too cold.

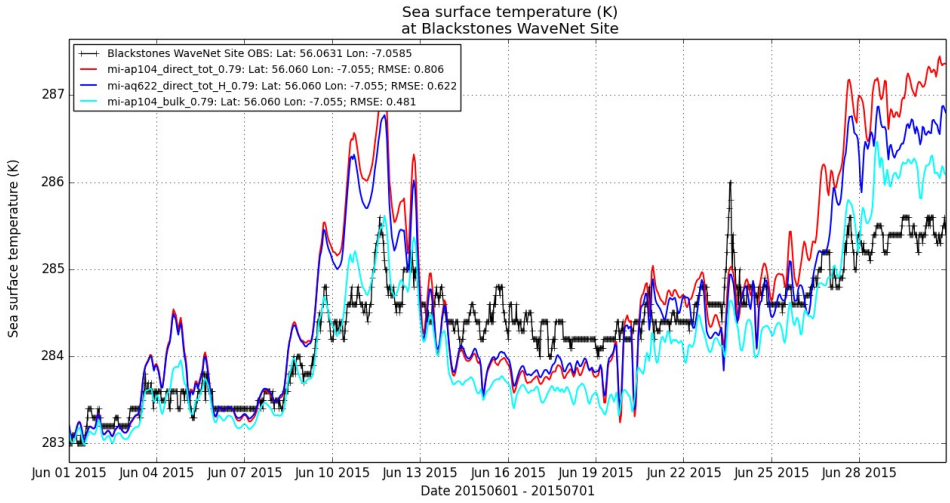

Figure 5. June 2015. Time series SST at Blackstones observation site. Red = NWP Direct QTot forced, Blue = NWP Direct QTot + Haney forced, Cyan = NWP bulk forced.

It should be noted however that in some areas adding Haney actually makes the direct forced run worse. This is true at the EAOW site for example (not shown), however overall when using Haney correction the SST from the direct forced run is significantly improved.

3.2 Partitioning the solar radiation input:

Figure 6 shows a spatial plot comparing the SSTs from using the differently partitioned solar radiation, with equivalent R-values. When using the Band 1 input, the SSTs are cooler over the whole domain than when using QTot. The choice of different R-values in these runs was intended to account for the different radiation components used, and so it is not immediately clear why results are so different. One consideration is the impact of atmospheric scattering/absorption impacting on the radiation at the ocean surface, compared with TOA assumptions (see also discussion in Appendix 3).

The time series plot shown in Figure 7 illustrates results found for a large proportion of the observation sites. The run using Band 1 is cooler than QTot but warmer than the bulk run, which gives relatively better agreement with the in-situ observations. However, results using Band 1 radiation appear to be quite volatile and very sensitive to sudden increases in temperature which affect the SST for this run significantly and increases the RMSE.

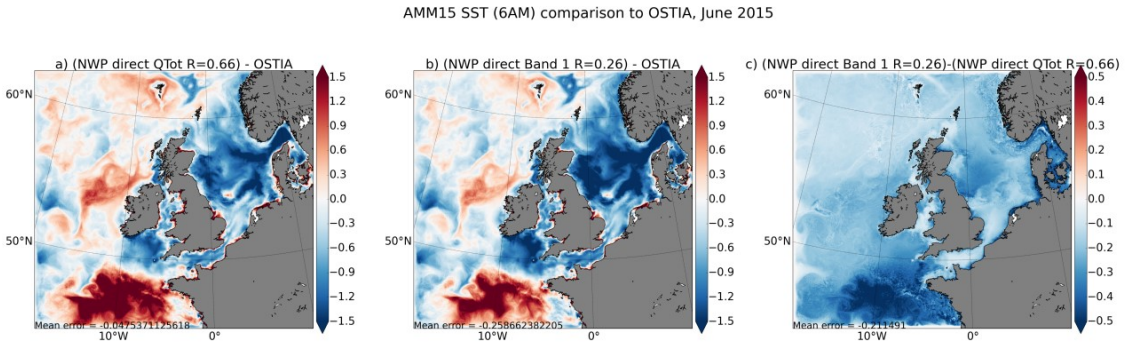

Figure 6. June 2015. SST comparisons with OSTIA. a) Direct QTot (R=0.66) - OSTIA, b) Direct Band 1 (R=0.26) - OSTIA, c) Direct (QTot – Band 1).

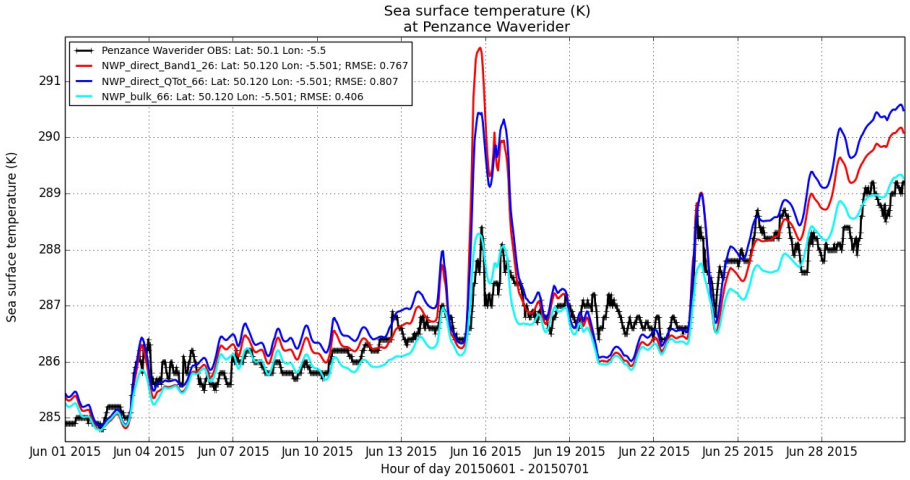

Figure 7. June 2015. SST from AMM15 run with direct (Band 1) forcing, direct forcing (QTot) forcing and bulk forcing. Red = Band 1, Blue = QTot, Cyan = bulk.

Both direct forced runs in Figure 7 exhibit a sensitivity to sharp increases in SSTs. This is not seen in the SST from the bulk forced configuration. This feature is also apparent in Figure 5, suggesting that with direct forcing the model tends to overshoot SSTs when a sudden temperature increase occurs.

As there is a difference in model SST between using Band 1 and QTot, QTot has been used for the remainder of the tests to investigate sensitivities to the R-value, as QTot is also used in the bulk forcing runs used for comparison.

3.3 Sensitivity to R-values

While recommended for improving results overall, the Haney correction was not applied in any of the tests comparing different R-values for direct forcing as this could influence the impact of changing the R-value, which is the focus of these experiments.

In areas where the waters are very well mixed and shallow, changing the fraction of penetrating shortwave radiation does not greatly affect the SST. This is seen for example in the southern North Sea, where the effect of changing the R-value is negligible (Figure 8 and Figure 9). The only instances where there are slight differences in SST traces between using different R-values occur where there are slight sharp increases in observed SST, due to strong heating i.e. shallow surface mixed layer. Here the SSTs from the different R-values separate out, with the lower R-value configuration SSTs increasing more than simulations with higher R-value. This effect is more evident in more seasonally stratified areas such as shown in Figure 10 and Figure 11.

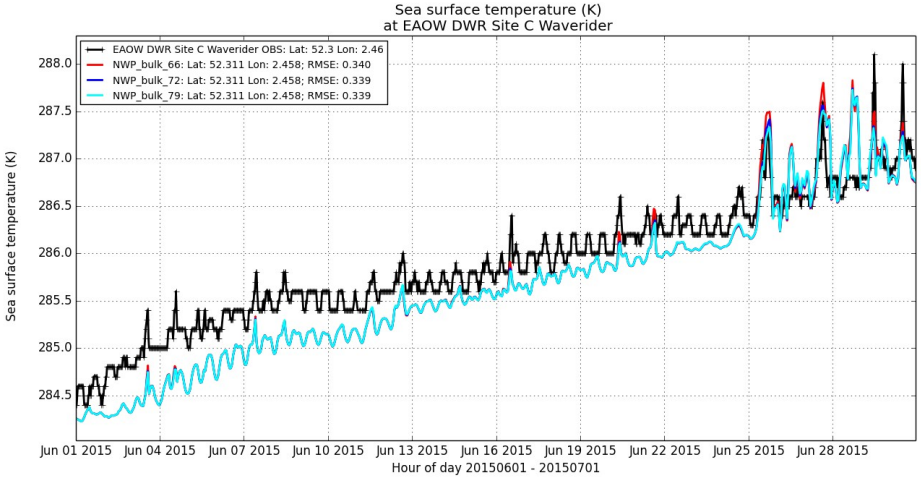

Figure 8. June 2015. Time series at EAOW. 3 different R values using NWP bulk forcing. R=0.66, Blue R=0.72, Cyan R=0.79.

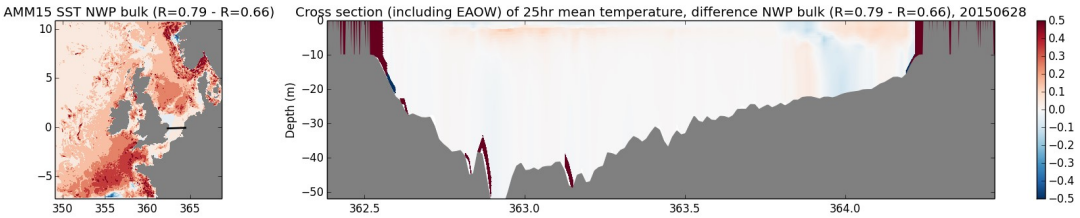

Figure 9. Cross section including EAOW station. Difference in temperature seen using NWP bulk forcing, R=0.79 - R=0.66. 28/06/2015.

Figure 10 show a time series of SST at the Tyne observation site in June 2015. This area is more stratified and the effect of varying the R-value can be seen – however it does not make a substantial difference to the SST comparison against observations. The model SST with R=0.79 is warmer overall compared to the configurations with lower R-values. With R=0.66, more of the incident shortwave solar radiation is allowed to penetrate the water column compared with R=0.79. This is evident in the cross section plot shown in Figure 11.

Additionally, it appears that with low R-values where more of the shortwave radiation is allowed to penetrate, when there is an increase in temperature sometimes as part of the diurnal cycle, the model SST rises sharply and then returns to follow the other traces. The other traces rise but not to the same extent.

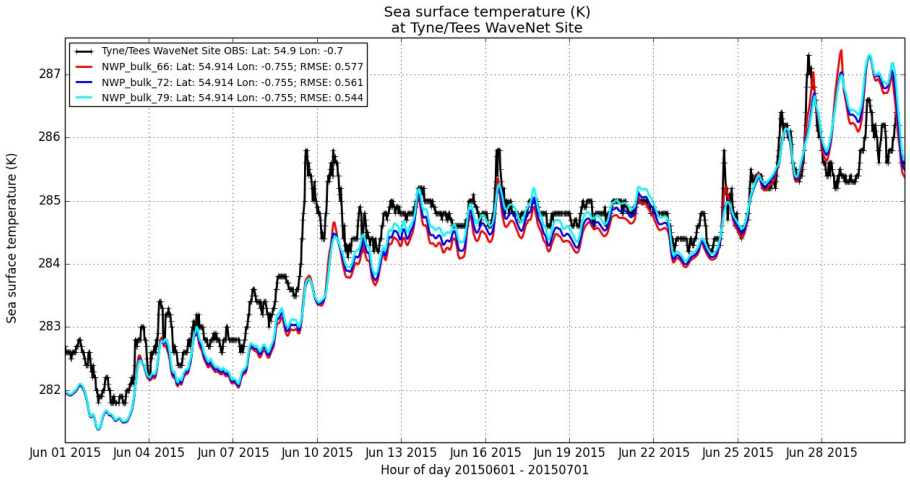

Figure 10. June 2015. Time series SST at Tyne site. 3 different R values, using bulk NWP forcing. Red R=0.66, Blue R=0.72, Cyan R=0.79.

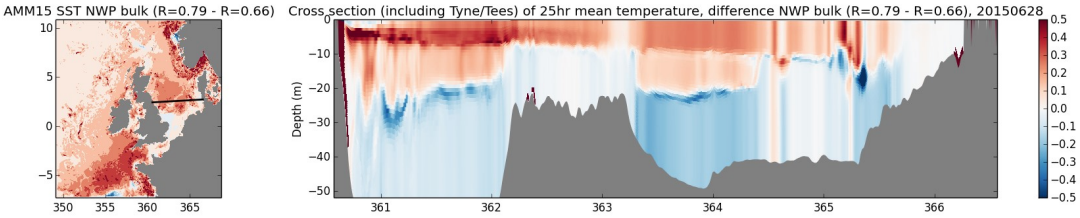

Figure 11. Cross section including Tyne/Tees station. Difference in temperature seen using NWP bulk forcing, R=0.79 - R=0.66. 28/06/2015.

Overall, when using direct forcing and changing the R-values, similar results can be obtained as shown when using bulk forcing. This is demonstrated in Figure 12, which compares the SST from using direct forcing and the three different R-values. Figure 12 also shows the effect of including the Haney correction. Again, in the instances where there are sudden jumps in SST, the use of different R-values becomes more apparent

(as it does in the tests using bulk forcing). A few more plots illustrating the 'jumps' which occur when using direct forcing are provided in Appendix 2. Although changing the R-value does not lead to large differences in SST for this area, the Haney corrected results are slightly closer to the observed SST values. This is seen clearly at Felixstowe (Figure 14) and most of the other observation stations.

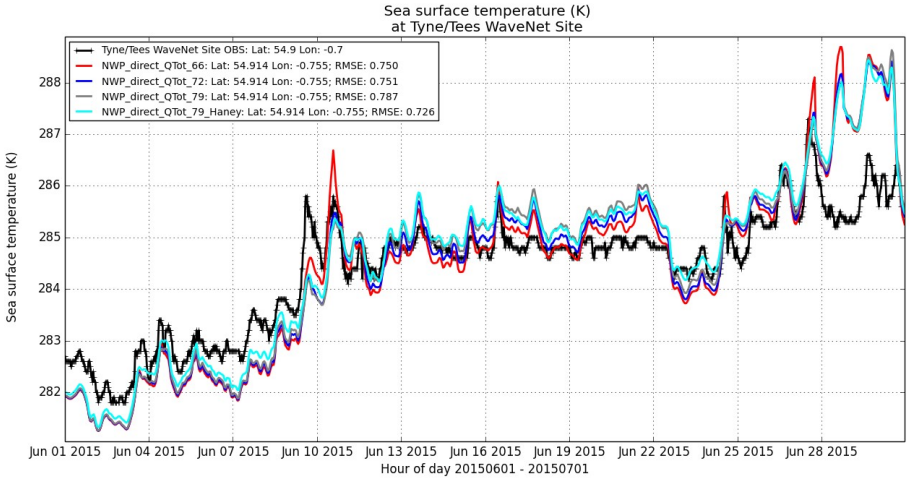

Figure 12. June 2015. Time series at Tyne observation site. Direct forcing with different R values. Effect of Haney correction shown. Red R=0.66, Blue R=0.72, Gray R=0.79, Cyan R=0.79 with Haney correction applied.

In the well mixed areas, different R-values have little effect on varying SST (see Figure 13), apart from where there are sudden increases in SST as was shown in Figure 12. The effect of adding in Haney correction is also evident in the well mixed areas (Figure 13 and Figure 14) where the R-values do not change SST, the Haney corrected trace stands apart from the other results, staying closer to the observed SST value for the majority of the month.

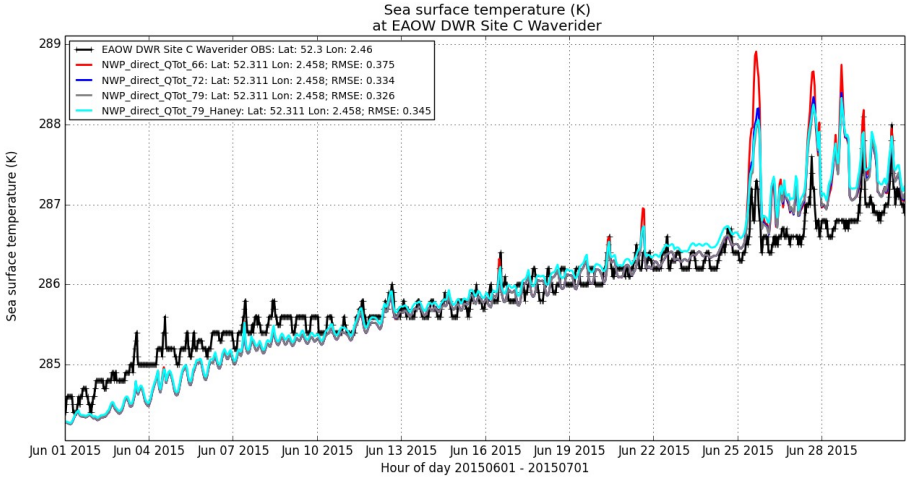

Figure 13. June 2015. Time series at EAOW. Different R values with direct NWP forcing. Red R=0.66, Blue R=0.72, Gray R=0.79, Cyan R=0.79 with Haney correction applied.

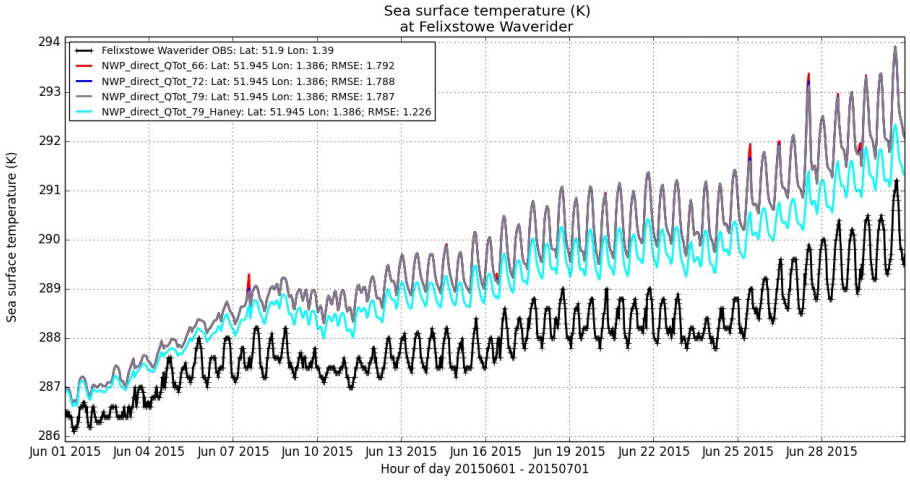

Figure 14. June 2015. Time series at Felixstowe. Different R values with direct NWP forcing. Red R=0.66, Blue R=0.72, Gray R=0.79, Cyan R=0.79 with Haney correction applied.

The effect of changing the R value is also demonstrated in the spatial plots of the whole AMM15 domain comparing the SSTs using R=0.79 and R=0.66 (Figure 15 and Figure 16). The SSTs were compared to OSTIA from running the model using bulk forcing with R=0.79 and R=0.66 (Figure 15a, Figure 15b) and the same but using Direct + QTot+Haney, (Figure 16a, Figure 16b). The difference in SSTs from using R=0.79 and R=0.66 for both bulk and Direct QTot + Haney forcing are shown in Figure 15c and Figure 16c respectively.

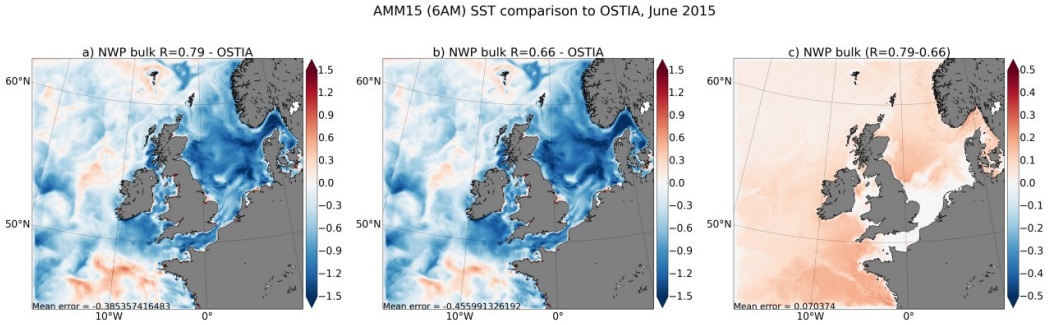

Figure 15. June 2015. SST comparisons with OSTIA. a) Bulk (R=0.79) - OSTIA, b) Bulk (R=0.66) - OSTIA, c) Bulk (R=0.79 - R=0.66).

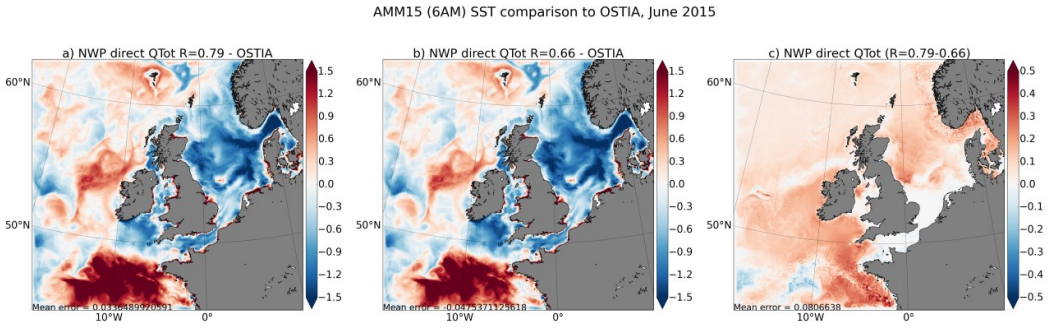

Figure 16. June 2015. SST comparisons with OSTIA. a) Direct QTot (R=0.79) - OSTIA, b) Direct QTot (R=0.66) - OSTIA, c) Direct QTot (R=0.79 - R=0.66).

Overall, Figure 15 and Figure 16 summarise the results from most of the tests carried out in this study. When compared to OSTIA, the bulk run has a cold bias and over most of the domain, the direct QTot run has a mostly warm bias, especially close to the coast. In addition to this, using a larger R-value does produce warmer SSTs than when using lower R-values – although not in areas that are well mixed such as the southern North Sea.

The differences in SST from runs using different R-values show up slightly more in the summer – but not greatly. A larger fraction of the incident solar radiation gets absorbed at the surface with larger R-values, and less warming further down the water column. This produces marginally warmer SSTs, of the order of +0.5K. It should be noted that these tests were carried out in June, and the effect may be more pronounced at the end of the summer.

Figure 17 shows the difference in temperature with depth, across 3 transects spanning the width of the AMM15 domain, on 30th June 2015 at the end of the trial summer month. These plots illustrate the how changing the R-value affects the temperature below the surface. The surface layers which are very responsive to solar heating are warmer when using a large R-value (R=0.79), however further down the water column at the top of the mixed layer there is a step change in temperature difference, where the run using a lower R-value (R=0.66) is warmer than when using a high R-value. This is due to a larger proportion of the solar radiation being allowed to penetrate beneath the surface with the lower R-value.

In shallow well mixed areas and close to the UK coast, overall the effect of different R-values is not very apparent. However further away from land, larger R-values produce

warmer temperatures close to the surface and cooler further down the water column. The same vertical pattern is seen when using direct forcing (plots not included).

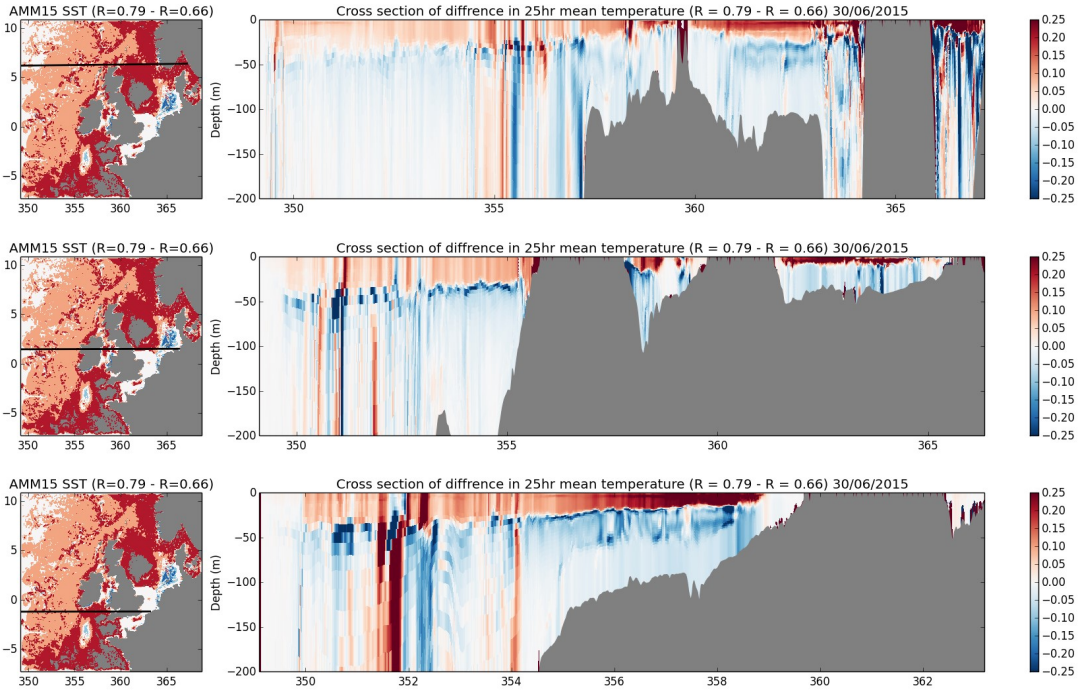

Figure 17. June 2015. Transects across different sections of AMM15 domain displaying the difference in vertical temperature distribution from running with R=0.79 and R=0.66. NWP bulk forcing was used.

The impact of varying the R-value in winter was also investigated, to confirm it had a less significant effect than in the summer as expected. A time series of SST using the highest and lowest R-value tested here with bulk forcing, at the Tyne observation site is shown in Figure 18. In the summer, changing the distribution of penetrating and non-penetrating light had an effect however in winter the difference is not apparent, as anticipated. The same is true for the SSTs in the southern North Sea (at the EAOW station, plot not shown). In this area, the jumps in SST associated with lower R-values in this area in summer are not seen in winter.

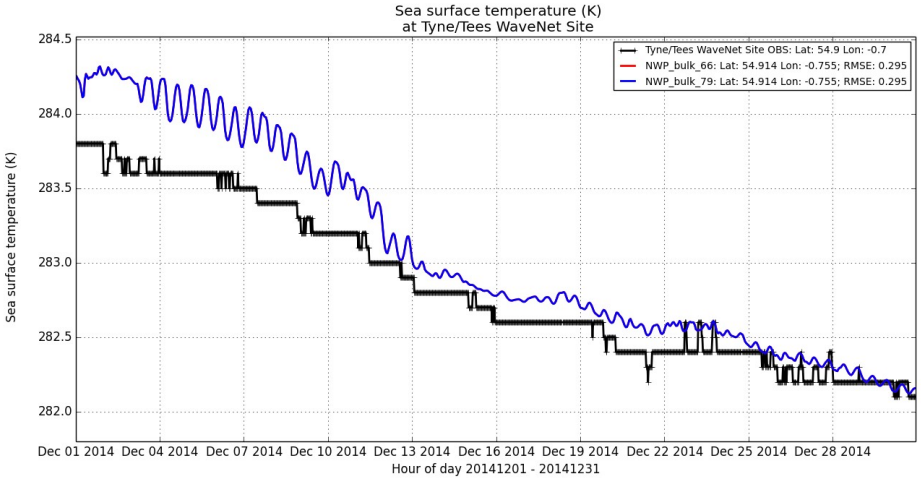

Figure 18. December 2014. Time series at Tyne site. Bulk NWP forcing with different R values. Red, R=0.66, Blue, R=0.79.

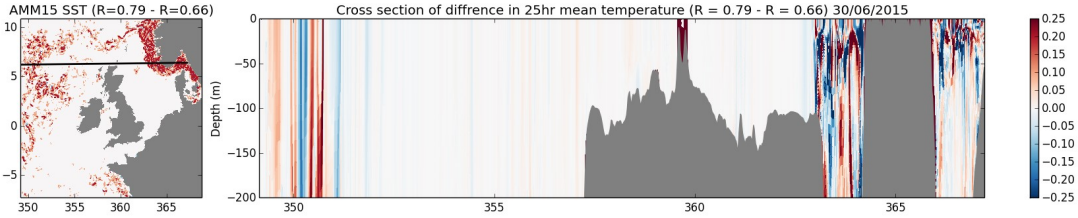

Figure 19. December 2014. Transects across different sections of AMM15 domain displaying the difference in vertical temperature distribution from running with R=0.79 and R=0.66. NWP bulk forcing was used.

This confirms what was expected. Figure 19 re-enforces the results shown in the time-series plot. In winter, on the shelf and in areas close to the coast, the R-value is not a large factor in determining SST. The areas which are affected by changes in the distribution solar radiation are limited to off the shelf and in the deep waters of the Atlantic and the Norwegian trench.

4. Conclusions

A series of different AMM15 ocean model configurations have been run over the months of December 2014 and June 2015, where the surface forcing method and the fractions of penetrating and non-penetrating solar radiation were changed to investigate the sensitivity of SST results to these choices.

Using bulk NWP fluxes to force the AMM15 model results in a slight cold bias relative to OSTIA and observations. This bias is more pronounced in summer than in winter (plot not shown). Using bulk forcing with ERA-Interim fluxes also shows good agreement compared to OSTIA and observations, however the bias is warm when using these fluxes. The direct forced run using NWP fluxes has a warm SST bias both in summer and winter. In winter the warm bias is more extreme than that seen when using bulk forcing with ERA-Interim fluxes. In summer using direct forcing appears to produce a warm patch in the south of the AMM15 domain.

It has been shown that forcing the AMM15 with direct QTot fluxes + Haney produces a much improved SST field compared to just forcing with Direct QTot.

Using the equivalent R-value for the model using QTot and using Band 1 as shortwave radiation input produces differences in SST. This may be due to differences in the treatment of the long wave radiation however this finding is unexpected and would benefit from further investigation. Although interesting, this outcome will not affect future test runs for UK Environmental Prediction research configurations, as these will all use the full shortwave radiation (QTot), in order to keep things as consistent as possible between different coupled/forced modes of simulations.

Altering the R-value has a small effect on the model SST. Larger R-values specify less penetrating radiation and when the AMM15 is run with these values, warmer SSTs are produced than when smaller R-values are used. This pattern is seen both when using bulk and with direct forcing. Lower R-values appear to make the SST more variable and volatile, and more sensitive to sudden temperature increases. However, this does not seem to greatly affect the model SST and after such an occurrence, it recovers to follow a similar evolution to that prior to the event.

In this study, only the SST has been evaluated in detail, but what happens further down the water column and to other fields should also be investigated to obtain a more complete picture of how the choice of R-value affect the ocean model. Before any strong conclusions are made concerning the effects of changing R-values, a longer simulation should also be run to understand impacts over a longer term.

Considering the results of the tests carried out here, the combination of forcing which produce the most stable SST is the NWP CORE forced run, using an R value of 0.79. The NWP CORE forcing does produce a cold SST bias, but from consideration of the time series plots, it appears to be relatively stable and consistently close to observations. If NWP direct forcing were to be chosen, Haney correction should be applied, as should an R-value of 0.79 with the total shortwave radiation (QTot) spectrum. This combination of parameters does produce SSTs with a warm bias (particularly off the shelf), and this is increased by a large R-value, but results are shown to be more stable with this value and less prone to sharp temperature jumps.

References:

Bell, M.J., Forbes, R.M., Hines, A., 2000: Assessment of the FOAM global data assimilation system for real-time operational ocean forecasting. J. Mar. Sys. 25 1–22

Dee D., Uppala, S., Simmons, A., Berrisford, P., Poli, P., Kobayashi, S., Andrae, U., Balmaseda, M., Balsamo, G., Bauer, P., et al.: The ERAI-Interim reanalysis: Configuration and performance of the data assimilation system, Quarterly Journal of the Royal Meteorological Society, 137, 553-597, 2011.

Donlon, C.J., M. Martin, J. D. Stark, J. Roberts-Jones, E. Fiedler and W. Wimmer, 2012. The Operational Sea Surface Temperature and Sea Ice Analysis (OSTIA), Rem. Sens. Env., 116, 140-158

Ford D., and Barciela R., 2015: Investigating biophysical feedbacks in a coupled physical-biogeochemical ocean model. Forecasting Research Technical Report No: 608

Graham, J. A., O'Dea, E., Holt, J., Polton, J., Hewitt, H. T., Furner, R., Guihou, K., Brereton, A., Arnold, A., Wakelin, S., Castillo Sanchez, J. M., and Mayorga Adame, C. G.: AMM15: a new high-resolution NEMO configuration for operational simulation of the European north-west shelf, Geosci. Model Dev., 11, 681-696, https://doi.org/10.5194/gmd-11-681-2018, 2018.

Haney, R. L.: Surface thermal boundary condition for ocean circulation models, Journal of Physical Oceanography, 1, 241–248, 1971.

Jerlov, N.G.,1951: Optical studies of ocean water. In: Rep. Swedish Deep-sea Exp. H. Pettersson, ed., 3(1), 1-69.

Large,W. G. and S. Yeager, 2004 : Diurnal to decadal global forcing for ocean and sea-ice models : the data sets and flux climatologies. NCAR Technical Note, NCAR/TN-460+STR, CGD Division of the National Center for Atmospheric Research.

Lengaigne, M., C. Menkes, O. Aumont, T. Gorgues, L. Bopp, and J.-M. A. G. Madec, 2007 : Bio-physical feedbacks on the tropical pacific climate in a coupled general circulation model. Clim. Dyn., 28, 503–516.

Lewis, H. W., Castillo Sanchez, J. M., Graham, J., Saulter, A., Bornemann, J., Arnold, A., Fallmann, J., Harris, C., Pearson, D., Ramsdale, S., Martínez-de la Torre, A., Bricheno, L., Blyth, E., Bell, V. A., Davies, H., Marthews, T. R., O'Neill, C., Rumbold, H., O'Dea, E., Brereton, A., Guihou, K., Hines, A., Butenschon, M., Dadson, S. J., Palmer, T., Holt, J., Reynard, N., Best, M., Edwards, J., and Siddorn, J.: The UKC2 regional coupled environmental prediction system, Geosci. Model Dev., 11, 1-42, https://doi.org/10.5194/gmd-11-1-2018, 2018.

O'Dea, E. J., Arnold, A. K., Edwards, K. P., Furner, R., Hyder, P., Martin, M. J., Siddorn, J. R., Storkey, D., While, J., Holt, J. T., and Liu, H.: An operational ocean forecast system incorporating NEMO and SST data assimilation for the tidally driven European North-West shelf, Journal of Operational Oceanography, 5, 3–17, 2012.

Madec, G.: NEMO ocean engine: Note Du Pôle de Modél, Institut Pierre-Simon Laplace (IPSL),France, No 27, ISSN No 1288-1619, 2008.

Morel, A., 1988 : Optical modeling of the upper ocean in relation to its biogenous matter content (case i waters). J. Geophys. Res, 93, 10,749–10,768.

Morel, A. and S. Maritorena, 2001 : Bio-optical properties of oceanic waters : a reappraisal. J. Geophys. Res, 106 (C4), 7163–7180.

Paulson, C. A. and J. J. Simpson, 1977 : Irradiance measurements in the upper ocean. J. Phys. Oceanogr., 7 (6), 952–956.

Stips A. K., 2010, Fitting measured irradiance of Jerlov water types to double exponential functions using R., JRG Tech. Notes (doi:10.2788/80912)

Storkey,D., E W Blockley, R Furner, C Guiavarc'h, D Lea, M J Martin, R M Barciela, A Hines, P Hyder & J R Siddorn (2010) Forecasting the ocean state using NEMO:The new FOAM system, Journal of Operational Oceanography, 3:1, 3-15, DOI: 10.1080/1755876X.2010.11020109

Walters, D. N., Williams, K. D., Boutle, I. A., Bushell, A. C., Edwards, J. M., Field, P. R., Lock, A. P., Morcrette, C. J., Stratton, R. A., Wilkinson, J. M., Willett, M. R., Bellouin, N., Bodas-Salcedo, A., Brooks, M. E., Copsey, D., Earnshaw, P. D., Harris, C. M., Levine, R. C., MacLachlan, C., Manners, J. C., Martin, G. M., Milton, S. F., Palmer, M. D., Roberts, M. J., Rodríguez, J. M., Tennant, W. J., and Vidale, P.: The Met Office Unified Model Global Atmosphere 4.0 and JULES Global Land 4.0 configurations, Geosci. Model Dev., 7, 35, 361–386, doi:10.5194/gmd-7-361-2014, 2014.

Previous Met Office work referenced:

Enda O'Dea: http://www-twiki/Main/ShelfSeasLightAttenuation

Dave Storkey: http://www-nwp/~frsy/papers_and_reports/pen_solar_radn.ps

John Edwards: see Appendix 3.

Appendix 1: Derivation of R-values

Diagram to explain calculation of equivalent Paulson and Simpson (P&S) R-values for Band 1 and QTot, based on one designed by Enda O'Dea (see http://www-twiki/Main/ShelfSeasLightAttenuation):

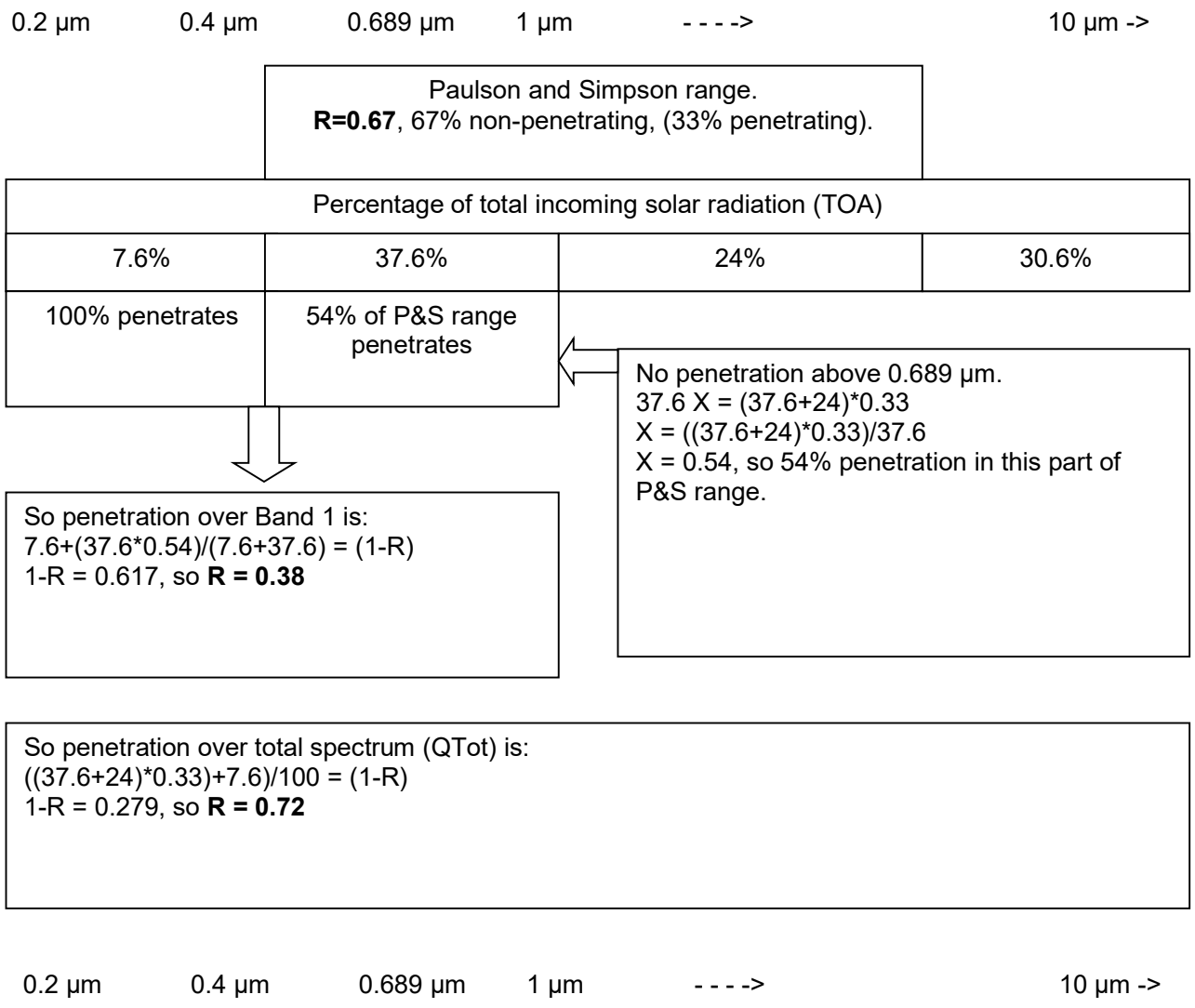

Appendix 2: Supplementary plots

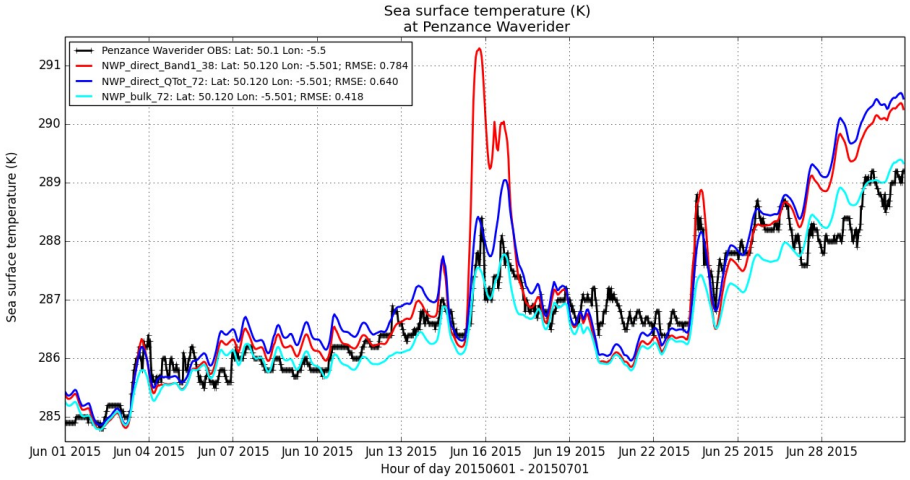

Figure 20. June 2015. Time series at Penzance site. Direct and bulk NWP forcing with different partitioning of solar radiation. Red = (Direct, Band 1, R=0.38), Blue = (Direct, QTot, R=0.72), Cyan = (Bulk, R=0.72).

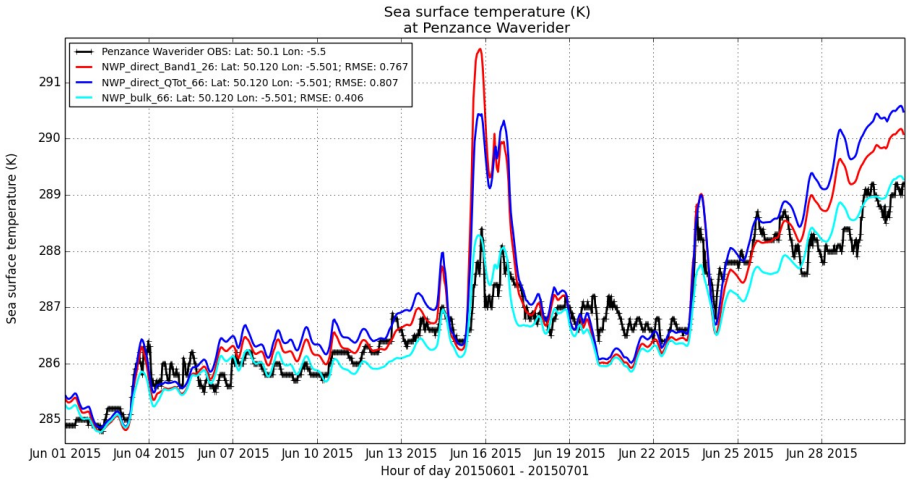

Figure 21. June 2015. Time series at Penzance site. Direct and bulk NWP forcing with different partitioning of solar radiation. Red = (Direct, Band 1, R=0.26), Blue = (Direct, QTot, R=0.66), Cyan = (Bulk, R=0.66).

Figure 20 and Figure 21 show time series of SST at Penzance. The SSTs in Figure 20 have been produced using R=0.38 and R=0.26 respectively for the Band 1 run. In both direct forced runs (Band1 and QTot), in both plots, the same jump in SST occurs around the 16th of June, where there is an increase in the observed SST.

This jump is not seen at all with the bulk forced run. Another point to note is that although there is a sudden increase in SST when using Band1, which is more extreme than when using QTot, the difference between which R-value is used is almost negligible for the Band 1 run, whereas it makes a difference to the extent to which the SST from QTot forced run increases by. The difference in QTot SST for the peak on the 16th June is ~2K (R=0.66 greater than R=0.72) but the difference in Band 1 SST for the same peak is only ~0.3K.

Appendix 3: Note by John Edwards on Ocean Optics (14/08/2013)

During the development of HadCM4, the question of how much radiation should penetrate into the ocean arose and evidence indicated that the penetration in HadCM3 was too low. The question has recurred periodically since then, so the following remarks, written at the time have been converted into a web-page for reference:

1. Paulson and Simpson's measurements for type IB water give an expression for the penetrating flux across the range of wavelengths 0.4-1.0 um:

   F/F_0 = 0.67 exp(z/1) + 0.33 exp(z/17)

2. In the UM flux across the whole range of solar wavelengths (effectively 0.2-5 um) is divided into `blue' and `red' components at 0.689 um. It is assumed that the `blue' component penetrates into the ocean with an exponential decay on a length-scale agreeing with the more penetrative term in the above formula (i.e. 17 m). The `red' component is put into the surface flux as it is absorbed so close to the surface. This can be related to the behaviour of the imaginary part of the refractive index of water which suggests stronger absorption beyond 0.7 um.

3. Typically in the model, the blue flux at the surface is about half the total flux, whereas the above formula might appear to suggest a figure of one third.

   Consider first fraction of the incident solar energy (at the TOA) in various wavelength regions:

0.2-0.4 um:	7.6%
0.4-0.689 um:	37.6%
0.689-1.0 um:	24.1%
1.0-10.0 um:	30.6%

at the TOA roughly 45% of the flux is blue and since longer wavelengths are generally absorbed more on descending through the atmosphere, it is not unreasonable that it should become a little more predominant at the surface, so the diagnosed figure of 50 % is not implausible. Further, there is a lot of flux outside the region measured by Paulson and Simpson.

Looking a little more closely at the optical properties of water it appears that there is no sharp change in the penetration depth at 0.7 um. Considering a plane wave propagating vertically downwards, the e-folding decay length should be

wavelength/(4*pi*Im(refractive_index))

For the region considered by Paulson and Simpson we therefore get

Wavelength (um)	Penetration Depth (m)
0.400000	17.1134
0.425000	26.0157
0.450000	35.1077
0.475000	40.4271
0.500000	39.7887
0.525000	31.6501
0.550000	22.3304
0.575000	12.7103
0.600000	4.38041
0.625000	3.57812
0.650000	3.15399
0.675000	2.40874
0.700000	1.66281
0.725000	0.630532
0.750000	0.382584
0.775000	0.416706
0.800000	0.509296
0.825000	0.360722
0.850000	0.230856
0.875000	0.178083
0.900000	0.147366
0.925000	0.0694426
0.950000	0.0258016
0.975000	0.0222954
1.00000	0.0275355

In practice, we would need to consider radiation travelling along a whole range of paths of different angles and allow for impurities, but these figures suggest that perhaps too much radiation is being allowed to penetrate into the ocean (a mean slant path for diffuse radiation would be inclined at 60 degrees to the vertical, halving the effective penetration depth). Because of the spread of penetration depths, the parameter R in the formula should not be seen as referring to a specific range of wavelengths, but merely as a fitted parameter. (One thing that does puzzle me is that Kraus as quoted in Table 2 of Paulson and Simpson gives a penetration depth of 40 m with a weight of 0.6 (1-R) for very clear water. On the basis of the above values the maximum pentration depth for vertical radiation is 40 m at just one wavelength, though the results for Type I water might be roughly consistent with this table).

Possible modifications:

The strict interpretation of the formula is that 33% of the incident radiation in the range 0.4-1.0 um should be allowed to penetrate. Using the TOA values above to get the weighting and noting that penetration depths are very shallow beyond 0.7 um, this would suggest that 54% of the radiation in the range 0.4-0.689 um should penetrate.

Supposing that all radiation at shorter wavelengths penetrates, it might seem more reasonable to allow 62% of the radiation in band 1 to penetrate, rather than all of it.

It might be possible to say something about the effect of the solar zenith angle. The fit above was derived for completely overcast conditions and should be appropriate for diffuse radiation. However, the omitted clear run (run 1) for which the sun was lower in the sky shows rather smaller irradiances. At depth the rate of decay is much the same as in the other runs, presumably because scattering in the ocean has made the radiance field fairly diffuse. But near the surface, where the light is still fairly collimated the decay is steeper as it must travel along a long slant path to reach any depth. However, this would require more thought.

Output from NEMO optical look-up table:

```
      IF(lwp) THEN
         WRITE(numout,*)
         WRITE(numout,*) 'trc_oce_rgb : Initialisation of the optical look-up table'
         WRITE(numout,*) '~~~~~~~~~~~ '
      ENDIF
      !
      !  Chlorophyll        !     Blue attenuation     !     Green attenuation    !     Red attenuation      !
      zrgb(1, 1) =  0.010   ;   zrgb(2, 1) = 0.01618   ;   zrgb(3, 1) = 0.07464   ;   zrgb(4, 1) = 0.37807
      zrgb(1, 2) =  0.011   ;   zrgb(2, 2) = 0.01654   ;   zrgb(3, 2) = 0.07480   ;   zrgb(4, 2) = 0.37823
      zrgb(1, 3) =  0.013   ;   zrgb(2, 3) = 0.01693   ;   zrgb(3, 3) = 0.07499   ;   zrgb(4, 3) = 0.37840
      zrgb(1, 4) =  0.014   ;   zrgb(2, 4) = 0.01736   ;   zrgb(3, 4) = 0.07518   ;   zrgb(4, 4) = 0.37859
      zrgb(1, 5) =  0.016   ;   zrgb(2, 5) = 0.01782   ;   zrgb(3, 5) = 0.07539   ;   zrgb(4, 5) = 0.37879
      zrgb(1, 6) =  0.018   ;   zrgb(2, 6) = 0.01831   ;   zrgb(3, 6) = 0.07562   ;   zrgb(4, 6) = 0.37900
      zrgb(1, 7) =  0.020   ;   zrgb(2, 7) = 0.01885   ;   zrgb(3, 7) = 0.07586   ;   zrgb(4, 7) = 0.37923
      zrgb(1, 8) =  0.022   ;   zrgb(2, 8) = 0.01943   ;   zrgb(3, 8) = 0.07613   ;   zrgb(4, 8) = 0.37948
      zrgb(1, 9) =  0.025   ;   zrgb(2, 9) = 0.02005   ;   zrgb(3, 9) = 0.07641   ;   zrgb(4, 9) = 0.37976
      zrgb(1,10) =  0.028   ;   zrgb(2,10) = 0.02073   ;   zrgb(3,10) = 0.07672   ;   zrgb(4,10) = 0.38005
      zrgb(1,11) =  0.032   ;   zrgb(2,11) = 0.02146   ;   zrgb(3,11) = 0.07705   ;   zrgb(4,11) = 0.38036
      zrgb(1,12) =  0.035   ;   zrgb(2,12) = 0.02224   ;   zrgb(3,12) = 0.07741   ;   zrgb(4,12) = 0.38070
      zrgb(1,13) =  0.040   ;   zrgb(2,13) = 0.02310   ;   zrgb(3,13) = 0.07780   ;   zrgb(4,13) = 0.38107
      zrgb(1,14) =  0.045   ;   zrgb(2,14) = 0.02402   ;   zrgb(3,14) = 0.07821   ;   zrgb(4,14) = 0.38146
      zrgb(1,15) =  0.050   ;   zrgb(2,15) = 0.02501   ;   zrgb(3,15) = 0.07866   ;   zrgb(4,15) = 0.38189
      zrgb(1,16) =  0.056   ;   zrgb(2,16) = 0.02608   ;   zrgb(3,16) = 0.07914   ;   zrgb(4,16) = 0.38235
```